1450–1460 *Nucleic Acids Research, 2010, Vol. 38, No. 5* *Published online 9 December 2009*
doi:10.1093/nar/gkp1074

A cassette of N-terminal amino acids of histone H2B are required for efficient cell survival, DNA repair and Swi/Snf binding in UV irradiated yeast

Ronita Nag, McKenna Kyriss, John W. Smerdon, John J. Wyrick and Michael J. Smerdon*

Biochemistry and Biophysics, School of Molecular Biosciences, Washington State University, Pullman, WA 99164-7520, USA

Received May 21, 2009; Revised November 1, 2009; Accepted November 3, 2009

ABSTRACT

The highly charged histone N-terminal domains are engaged in inter- and intra-nucleosomal interactions, and contain a host of sites used for post-translational modification. We have studied the effect of deleting residues 30–37 from the N-terminal domain of histone H2B in yeast cells, on nucleotide excision repair (NER) following UV irradiation, as these cells are quite sensitive to UV. We find that H2B Δ30–37 cells exhibit reduced NER efficiency at three specific chromatin loci: the transcriptionally active, *RPB2* locus; the transcriptionally silenced, nucleosome-loaded *HML* locus; and the transcriptionally repressed, non-silenced, *GAL10* locus. Nuclease digestion studies indicate that H2B Δ30–37 chromatin has increased nucleosome accessibility and/or nucleosome mobility. In addition, H2B Δ30–37 mutants acquire more DNA damage, compared to *wt* cells, following the same dose of UV radiation. Reducing the level of damage in H2B Δ30–37 cells to match that of *wt* cells restores the NER rate to *wt* levels in the *RPB2* and *GAL10* loci, but NER efficiency remains low in the silenced *HML* locus. Interestingly, recruitment of Snf5 to the *HML* locus is reduced in H2B Δ30–37 cells and more transient following UV irradiation. This may reflect a lower binding affinity of the SWI/SNF complex to H2B Δ30–37 nucleosomes.

INTRODUCTION

DNA in eukaryotic cells is compacted into chromatin, through association with histone proteins. Nucleosomes, the fundamental units of chromatin, are composed of an octamer of four core histones, H3, H4, H2A and H2B around which ~147 base pairs of DNA are wrapped. Each core histone comprises a histone-fold domain that contributes to the central spool around which the DNA wraps, and an N-terminal domain that projects beyond the DNA gyres towards the outside of the nucleosome (1,2). For different DNA processing events to occur in the cell nucleus, the chromatin needs to be dynamic and allow modifications both at the level of single nucleosomes and at higher levels of nucleosome compaction. The histone proteins, especially the N-terminal domains, are important regulators of chromatin structure and consequently DNA accessibility during vital cellular functions. The N-terminal domains not only engage in inter- and intra-nucleosomal histone–DNA interactions needed to stabilize chromatin structure, but also provide sites for numerous posttranslational modifications that occur during DNA metabolism (3–5). The ultimate effect of most histone tail modifications is disruption of the structural stability of chromatin in order to expose required sites for functions (6–8). As most posttranslational modifications target either an individual core histone tail or a subset of these tails, it can be presumed that the histone tails contribute largely toward regulation of the structural and functional state of the chromatin fibers. In fact, several *in vitro* studies have shown that the core histone tails interact with DNA in the linker regions between nucleosome core particles, and with inter-nucleosomal DNA (3,9). These interactions might contribute to the formation of higher order chromatin structure (10). Furthermore, alterations in the histone tail domains can affect nucleosome mobility and dynamics, sequence-dependent nucleosome positioning and ATP-dependent nucleosome remodeling (11–14).

The histone H2B N-terminal tail, along with that of histone H3, is known to pass between the two gyres of the DNA superhelix, and the highly basic H2B tail is predicted to be involved in higher order chromatin formation

*To whom correspondence should be addressed. Tel: +1 509 335 6853; Fax: +1 509 335 9688; Email: smerdon@wsu.edu

through inter-nucleosomal interactions (2). The H2B N-terminal domain contains an extremely basic eight amino acid stretch, which passes through the aligned minor grooves of the DNA superhelix near SHL −3 and +5. In this basic span, the main chain amide nitrogen of H2B S-33 is known to make hydrogen bonds with the phosphate backbone of DNA (2). More recent biophysical studies on nucleosome structure has confirmed that the proximal domain of the histone H2B N-terminal tail interacts with the DNA minor groove when passing between the two gyres close to SHL +5, and this may serve to stabilize octamer positioning on the DNA (15,16). Consistent with these observations, is the finding that the histone H2B N-terminal tail regulates translational positioning of nucleosomes, and deletion of the first 20 amino acids from the H2B tail causes increased nucleosome sliding along the DNA (11). Moreover, the observations that chromatin remodeling complex Swi/Snf targets the H2B N-terminal region (17) and removal of the H2A/H2B N-tail significantly facilitate nucleosome traversal by RNA Pol II (18) further strengthens the idea that the H2B N-terminus is a strong regulator of chromatin structure and function.

Mutation or deletion of H2B N-terminal domain residues have been shown to cause UV sensitivity (19), along with other phenotypes like derepression of basal transcription at certain chromatin loci, transcriptional up-regulation of 8.6% of yeast genes and alleviation of the need for Swi/Snf during transcription (17,19,20). Therefore, we reasoned that H2B N-terminal deletion mutants could provide insights into the correlations between chromatin structure and DNA repair. Here we discuss the effect of deleting amino acids 30–37 (KKRSKARK) from the N-terminus of histone H2B, on NER and chromatin structure. We find that H2B Δ30–37 mutants have reduced NER efficiency at certain chromatin loci and accumulate more UV-induced DNA damage, compared to wild type cells. Furthermore, nucleosomes in the mutant chromatin have increased accessibility and/or mobility and Snf5 occupancy in specific chromatin regions of the mutant cells is reduced and more transient during NER. The combination of altered chromatin structure, increased UV-induced DNA damage, and the inability of H2B Δ30–37 mutant nucleosomes to recruit Snf5 efficiently, may contribute to the high UV sensitivity observed in these cells.

MATERIALS AND METHODS

Locus-specific DNA damage and repair analyses

NruI, Bsp1286I and EcoRI–EcoRV were used to release the 3.4 kb fragment containing the *RPB2* gene, the 2.3 kb fragment from the *HML* locus and the 2.2 kb fragment of the *GAL10* locus, respectively. The number of CPDs in specific restriction fragments was determined as described previously (21,22). Briefly, equal amounts of purified and restriction-digested DNA were either mock-treated or treated with T4 endonuclease V for 60 min at 37°C. DNA was denatured and electrophoresed on 1% alkaline agarose gels, transferred to Hybond N^+ membranes, and hybridized with specific radioactive DNA or RNA probes. The probes for *RPB2* locus were generated using linearized plasmid pKS212 (23). For the *HML* locus, a fragment representing nucleotides +1 to +518 was generated from the *HMLα1* ORF by PCR amplification. For the *GAL10* probe a fragment representing +1 to +800 bp relative to the start site was used. The fragments were radiolabeled using [α^{32}P]dATP and the Prime-It Random Primer Kit (Stratagene). Southern blots were quantified using PhosphorImager and IMAGE-QUANT software (GE Healthcare). The level of DNA damage and repair was calculated as from the average amount of CPDs remaining per fragment, assuming a Poisson distribution (23,24).

Immuno-slotblot assay

To quantify genomic CPD and 6-4PPs, each strain was exposed to different doses of UV light (254 nm). Genomic DNA was prepared as described earlier. Equal amounts of DNA for each UV dose, were denatured by adding 0.4 N NaOH and then boiling the samples for 5 min. The samples were then brought to a volume of 200 µl by adding 10× SSC and applied to Hybond N+ transfer membrane (Amersham) in triplicate using BIO-DOT SF (Biorad). UV radiation-induced photoproducts in the genomic DNA were examined by western blotting with monoclonal CPD or 6-4PPs antibodies (25) followed by a secondary antibody/horseradish peroxidase conjugate. This secondary antibody was detected with ECL Plus Western Blotting Detection System (GE Healthcare). Western blots were scanned using a STORM 840 Fluorescence-Imager (GE Healthcare) and quantified using IMAGE-QUANT software (GE Healthcare). Southern blot analyses were then performed on the same membranes with random genomic probes to correct for loading differences between slots. Western blot signals were then normalized with the corresponding Southern blot signals to yield relative numbers of CPDs and 6-4PPs for each strain.

Chromatin accessibility assay

Micrococcal nuclease (MNase) digestion was done following protocols as described previously (24). Briefly, spheroplasts were prepared from 100 ml of mid-log phase ($\sim 1.0-2.0 \times 10^7$ cells/ml) yeast cells incubated for 20 min in 1 ml of YLE (10 mg/ml Zymolyase in 1 M Sorbitol and 5 mM β-mercaptoethanol) at room temperature and then washed twice with Sorbitol wash buffer (1 M Sorbitol, 1 mM PMSF, 2 mM β-mercaptoethanol). Spheroplasts were then suspended in spheroplast digestion buffer (1 M Sorbitol, 50 mM NaCl, 10 mM Tris–HCl, pH 7.5, 5 mM $MgCl_2$, 1 mM $CaCl_2$, 1 mM β-mercaptoethanol, 0.5 mM spermidine and 0.075% v/v NP-40), divided into 200 µl aliquots and digested with varying concentrations of MNase (10 U/µl) for 10 min at 37°C. The reactions were terminated with 0.1 volume of stop solution (5% SDS, 250 mM EDTA) followed by Proteinase-K treatment for 2 h at 55°C. Samples were extracted twice with phenol : chloroform, treated with 5 µg/ml of RNase A and

ethanol precipitated. DNA was resuspended in TE (10 mM Tris pH 8.0, 1 mM EDTA) and electrophoresed on 1.2% agarose gels. Southern blots were done with random primed ^{32}P-labeled probes specific for *HML* or *RPB2* locus.

Chromatin immunoprecipitation

Chromatin immunoprecipitation (ChIP) was performed as described by Kuo and Allis (26). Mid-log phase yeast cells were treated with 1% formaldehyde for 20 min at room temperature, pelleted and washed twice with TBS (25 mM Tris, pH 7.5, 137 mM NaCl, 2.7 mM KCl). Crosslinked cells were suspended in lysis buffer (50 mM HEPES–KOH, pH 7.5, 140 mM NaCl, 1 mM EDTA, 1% Triton X-100, 0.1% sodium deoxycholate, 1 mM PMSF, 1 mg/ml leupeptin, 1 mg/ml pepstatin A) and disrupted using glass beads (425–600 μm, Sigma), followed by sonication. Protein levels in the extract were estimated using the Bradford assay. Equal amounts of protein from each sample were used for immunoprecipitation with anti-Snf5 antibody (Abcam: ab24425). The reaction mixture was incubated overnight at 4°C, and the immunocomplex precipitated using Protein A sepharose beads (50% slurry). The beads were consecutively washed with lysis buffer, wash buffer 1 (Lysis buffer containing 500 mM NaCl), wash buffer 2 (10 mM Tris–HCl, pH 8, 250 mM LiCl, 0.5% NP-40, 0.5% sodium deoxycholate, 1 mM EDTA) and TE buffer and then treated with RNase A in TE at 37°C for 30 min. Chromatin was then eluted from the beads using elution buffer (1% SDS, 0.1 M $NaHCO_3$) and the crosslinks reversed by incubation at 65°C overnight. Fragments representing specific loci were amplified from the immunoprecipitated DNA using gene-specific primers and PCR. PCR products were resolved on 1.5% agarose gels and the signals quantified using IMAGE-QUANT software (GE Healthcare).

To examine histone occupancy at the *HML* locus, chromatin immunoprecipitation was performed essentially as described above using an anti-H2B antibody (Active Motif; 39237) or anti-H3 antibody (Abcam; ab46765). Three gene-specific primer sets were used to measure H2B and H3 content in the *HML* locus: primer set A (5′-AGTTTTCGGCACGGACTTATTTGG-3′ and 5′-TCGTCTAATACAAGTTTGAATGACG-3′; 27), primer set B (5′-GATGCAATTTATTGCTTCCC-3′ and 5′- CATATTGTGAATGTCGTC-3′; 27) and primer set C (5′-CGCGGACAAAATGCAGCACG-3′ and 5′-CCGTCACCACGTACTTCAGC-3′; this study). PCR products of these three primer sets were normalized to the level of control PCR product amplified from the *ACT1* locus (5′-AAACTCGCCTCTCTCTCTC-3′ and 5′-GATGGTGCAAGCGCTAGAA-3′; this study). PCR products were resolved on 2% agarose gels, stained with ethidium bromide, and quantified using a GelDoc EQ imager and Quantity One software (Bio-Rad). The final enrichment value was calculated by comparing the *HML* specific PCR product enrichment relative to *ACT1* in the immunoprecipitated samples versus the whole cell extract (input) samples (28).

Western blot

Total cellular protein was isolated using the trichloroacetic acid precipitation method. The protein samples were resolved by 10% SDS–PAGE and blotted onto Immunoblot-PVDF membrane (BIORAD). The blots were probed with α-Snf5 antibody (Abcam: ab24425) and α-tubulin antibody (Abcam, ab-6160), respectively, followed by a secondary antibody/horseradish peroxidase conjugate. This secondary antibody was detected with ECL Plus Western Blotting Detection System (GE Healthcare). The blots were scanned using a STORM 840 Fluorescence-Imager (GE Healthcare) and quantified using IMAGE-QUANT software (GE Healthcare).

RESULTS

We have measured the effect of deleting amino acids 30–37 in the histone H2B N-terminal domain on NER of UV-induced DNA damage and on regulation of chromatin structure. The H2B Δ30–37 mutant strain was generated by plasmid shuffling into a wild type (*wt*) yeast strain, in which the four chromosomal copies of H2A and H2B histone genes have been sequentially deleted, and the *wt* or mutant H2B gene was expressed on a plasmid (19). The H2B Δ30–37 mutant strain was previously reported to be sensitive to UV radiation, with an ∼100-fold lower survival rate compared to *wt* cells, when irradiated with a UV dose of 100 J/m^2 (19). Here, we set out to determine the underlying cause of this increased UV sensitivity phenotype.

NER efficiency in different chromatin regions of H2B Δ30–37 mutant cells

For NER studies, yeast cells were irradiated with 254 nm UV light (100 J/m^2), incubated for different repair times, and the removal of *cis-syn* cyclobutane pyrimidine dimers (CPDs) was monitored using T4 endonuclease V (T4 endo V) digestion, which nicks DNA 5′ to CPDs, as we previously described (24). Based on their chromatin structure, three different kinds of loci in yeast were examined: (i) the nucleosome-loaded and silenced mating-type locus *HML*; (ii) the constitutively transcribed, *RPB2* gene; and (iii) the nucleosome-loaded, inducible *GAL10* locus under transcriptionally repressed conditions.

Repair of CPDs in the *HML* locus was monitored in a 2.38 kb *Bsp*1286I fragment (Figure 1A). As shown in Figure 1B, CPD removal is less efficient in the mutant cells than *wt*. For example, after 1 h of repair ∼70% of the CPDs are removed from *wt* cells, as compared to only 40% in the mutant cells. Similar results were obtained when CPD removal was examined in the 3.4 kb NruI fragment containing the *RPB2* locus or the 2.2 kb EcoRI–EcoRV fragment containing the *GAL10* gene (Figure 1C–F). Although the repair difference between the *wt* and the H2B Δ30–37 cells varies between the different loci, the mutant clearly exhibits a slower NER rate in each case. Together with the results of Parra *et al.* (19), these results indicate that the reduced rate of CPD repair in the H2B Δ30–37 mutant cells contributes, at least

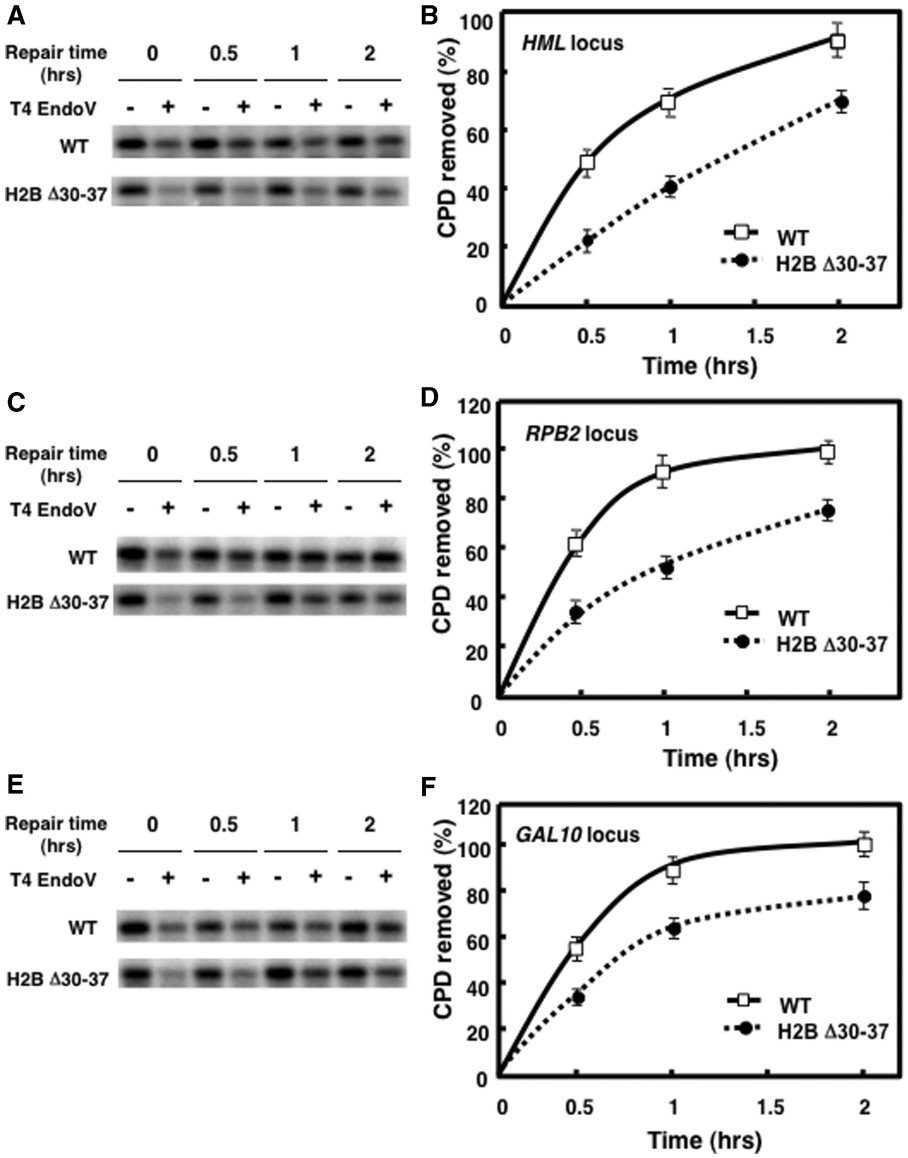

Figure 1. NER in the *HML, RPB2* and *GAL10* loci. For repair experiments, cells were UV irradiated (100 J/m^2) and incubated in the dark for various time periods (0.5–2 h). Genomic DNA was isolated, digested with appropriate restriction enzymes and then digested to completion with T4 endo V. Southern analyses were performed using radiolabeled probes specific for *HML, RPB2* and *GAL10* loci. Representative alkaline agarose gels used for CPD content (T4 endo V cutting) in the 2.3 kb *Bsp*1286I fragment (*HML*), 2.2 kb EcoRI–EcoRV fragment (*GAL10*) and the 3.4 kb *Nru*I fragment (*RPB2*) are shown in (**A**, **C** and **E**), respectively. The time courses calculated for CPD removal from the *HML, RPB2* and *GAL10* loci are shown in (**B, D** and **F**), respectively. For each strain, data represent the mean ± 1 SD for three independent experiments.

in part, to the increased UV sensitivity observed in these cells.

Deletion of H2B residues 30–37 affects DNA damage formation

The reduced NER efficiency exhibited by the H2B Δ30–37 mutant cells could reflect a greater UV photoproduct yield in these cells compared to *wt*. Therefore, both mutant and *wt* cells were irradiated with increasing doses of UV and the levels of CPD formation were determined in the three chromatin loci examined above. As shown in Figure 2, CPD formation was distinctly higher in the H2B Δ30–37 mutant cells at all three loci, with the difference being most apparent in the 3.4 kb fragment of the *RPB2* locus (Figure 2B). For example, at a UV dose of 100 J/m^2 the number of CPDs formed in the *RPB2* locus of the mutant cells (~1.6 per fragment) is almost 2-fold higher than in the *wt* cells (~0.8 per fragment). Similarly, the H2B Δ30–37 cells acquired more CPDs (~1.2 per fragment) in the *GAL10* locus, compared to *wt* (~0.7 per fragment), at 100 J/m^2 (Figure 2C). The smallest, albeit statistically significant ($P < 0.05$), difference in CPD formation between the *wt* and mutant cells was observed in the 2.4 kb fragment at the *HML* locus (Figure 2A), where the mutant cells acquired about 1.3-fold more CPDs at 100 J/m^2.

Since the yield of UV-induced CPDs in H2B Δ30–37 mutant cells was higher than in *wt* cells at three different

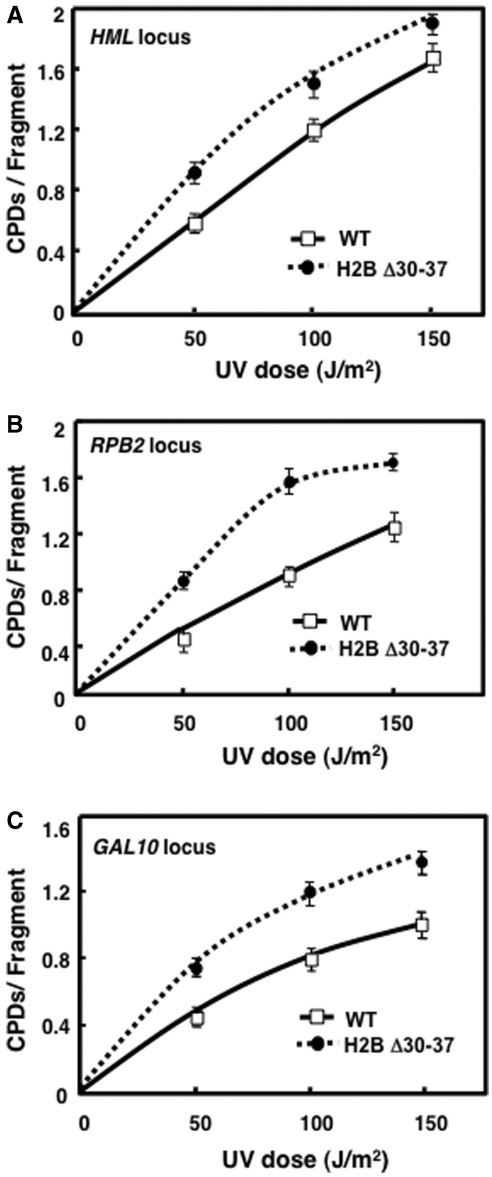

Figure 2. CPD formation in the *HML, RPB2* and *GAL10* loci. For quantification of CPDs, cells were irradiated with increasing UV doses, harvested immediately and the genomic DNA was digested to completion with T4 endo V. Southern analyses was performed using radiolabeled probes specific for *RPB2, GAL10* and *HML* loci, respectively. Graphic-representation of the number of CPDs formed per fragment of the *RPB2, GAL10* and *HML* loci are shown in (**A, B** and **C**), respectively. For each strain, data represent the mean ± 1 SD for three independent experiments.

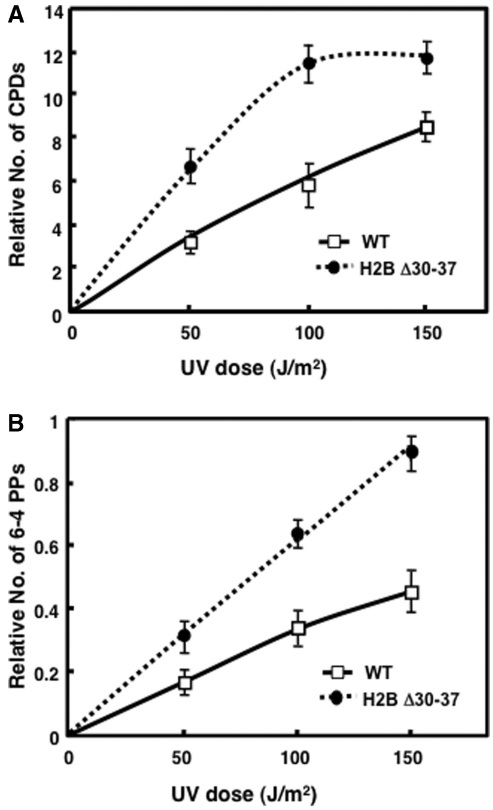

Figure 3. CPD and 6-4 photoproduct formation in total genome DNA. For total genome CPD and 6-4 photoproduct quantifications, cells were UV irradiated as mentioned in the legend to Figure 2 and the genomic DNA was subjected to slot blot hybridization with antibodies specific to CPDs or 6-4PPs. Southern analysis of the same membrane was used to correct for loading differences between slots and yield the relative number of CPDs and 6-4PPs for each strain. Graphical representation of the number of CPDs and 6-4PPs formed in the genome are shown in (**A** and **B**), respectively. For each strain, data represent the mean ± 1 SD for three independent experiments.

chromatin loci, we measured the total genome levels of the two major UV photoproducts in DNA [CPDs and pyrimidine (6-4) pyrimidones, or (6-4)PPs]. Both *wt* and mutant cells were irradiated with increasing UV doses, and the levels of CPDs and (6-4)PPs were measured using antibodies specific for these lesions. As shown in Figure 3A and B, at similar UV doses the H2B Δ30–37 mutant chromatin accumulates a significantly higher number of UV-induced DNA lesions, both CPDs and (6-4)PPs, when compared to *wt*. For example, at a UV dose of 100 J/m^2, the yield of CPDs and (6-4)PPs was ~2-fold higher in the H2B Δ30–37 mutant cells, compared to *wt*.

Comparable DNA damage levels yield *wt* NER efficiencies in the 'open loci' of H2B Δ30–37 mutant cells

To test the possibility that the increased level of UV damage in H2B Δ30–37 mutants is responsible for their reduced NER rate, we irradiated H2B Δ30–37 cells with a lower UV dose (70 J/m^2) than *wt* (100 J/m^2) and examined NER in the three specific loci mentioned above. As shown in Figure 4A, the rate of NER in the transcriptionally silent *HML* locus remains lower than *wt* in H2B Δ30–37 cells, even with similar levels of CPDs (Figure 4A). On the other hand, at the lower UV dose, the rate of NER in both *RPB2* and *GAL10* loci of H2B Δ30–37 cells becomes similar to that of the *wt* cells (Figure 4B and C). These results indicate that in the *HML* locus of the H2B Δ30–37 mutant cells, the impaired NER rate observed is not just due to higher levels of UV-induced DNA damage.

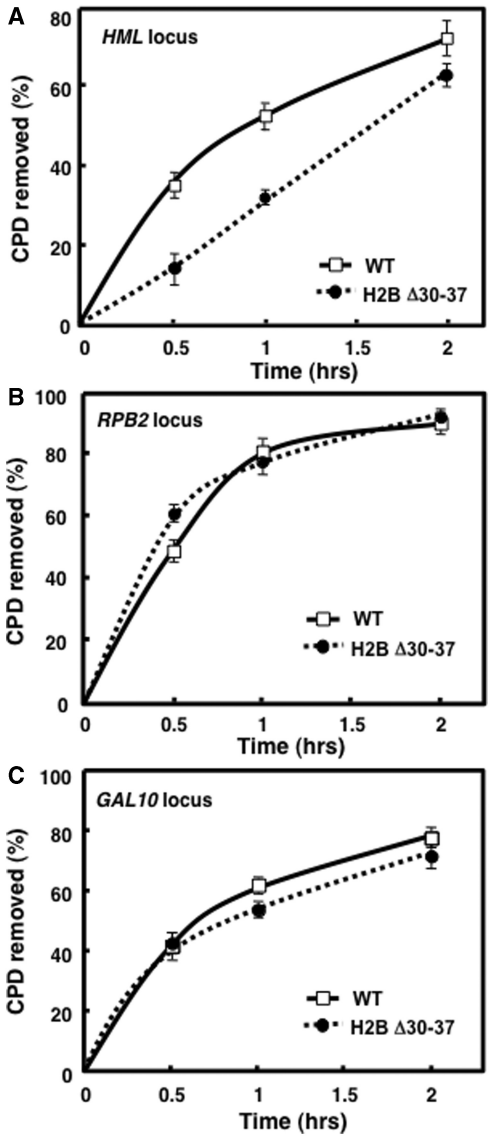

Figure 4. NER in H2B Δ30–37 mutant cells with similar DNA damage levels as *wt* cells. H2B Δ30–37 and *wt* cells were irradiated at UV doses of 70 J/m^2 and 100 J/m^2, respectively, followed by repair incubations. Genomic DNA was then digested with locus specific restriction enzymes followed by T4 endo V digestions, as mentioned earlier. Graphical representation of CPD removal from the *RPB2*, *GAL10* and *HML* loci are (**A, B** and **C**), respectively. For each strain, data represent the mean ± 1 SD for three independent experiments.

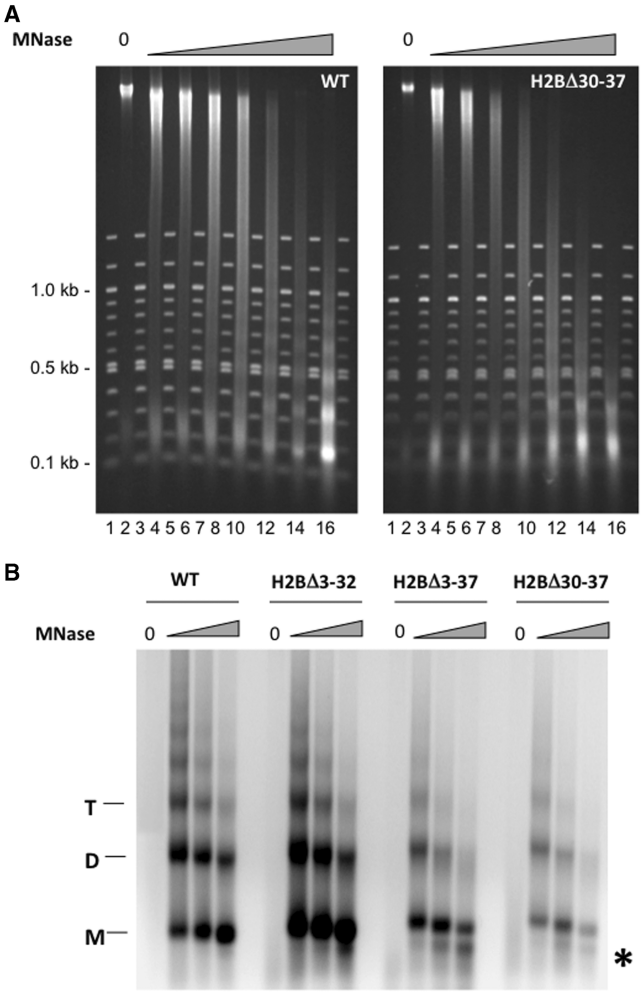

Figure 5. MNase digestion patterns for H2B mutant chromatin. (**A**) Isolated spheroplasts from *wt* and H2B Δ30–37 cells were treated with different concentrations of MNase, as described in 'Materials and Methods' section, and genomic DNA was isolated and separated on 1.2% agarose gels, with 100 bp repeat marker fragments (New England Biolabs) run in every other lane to facilitate measurements of nucleosome repeat lengths. Digestion profiles of bulk chromatin were stained with ethidium bromide. (**B**) Isolated spheroplasts from *wt*, H2B Δ3–32, H2B Δ3–37 and H2B Δ30–37 cells were treated with different concentrations of MNase, genomic DNA was isolated and then separated on 1.2% agarose gels. M, D and T denote positions of mono-, di- and tri-nucleosome DNA populations, respectively. The position of a prominent sub-monomer band in the mutant chromatin digest is denoted with a '*'.

Nuclease digestion studies on chromatin from H2B Δ30–37 mutant cells

Earlier studies established that chromatin structure could affect DNA damage formation and the rate of NER (29). Thus, the higher damage accumulation in H2B Δ30–37 mutant cells could reflect an altered chromatin structure in these cells. We examined the micrococcal nuclease (MNase) accessibility of DNA in the bulk chromatin of H2B Δ30–37 mutant cells compared to *wt*. The MNase digestion patterns show that nucleosome DNA in the H2B Δ30–37 mutant chromatin is more accessible than in *wt* (Figure 5). As shown in Figure 5A, the same MNase digestion conditions that yield a distinct nucleosome ladder of up to 6–7 repeats for *wt* cells generate only 3–4 repeats in the chromatin of H2B Δ30–37 cells, with a higher background of randomly cut (or smeared) DNA between bands (Figure 5A, compare lanes 12, 14 and 16 of the two gels). This result indicates that in mutant chromatin the nucleosomes may be more mobile compared to *wt*.

We also performed MNase digestions with chromatin from H2B Δ3–32 and H2B Δ3–37 cells. Our results show that similar to *wt* chromatin, H2B Δ3–32 chromatin yields a distinct nucleosome ladder, while both H2B Δ3–37 and H2B Δ30–37 nucleosome ladders have similar, less distinct, characteristics (Figure 5B). Moreover, like H2B Δ30–37 chromatin, MNase digests of H2B Δ3–37

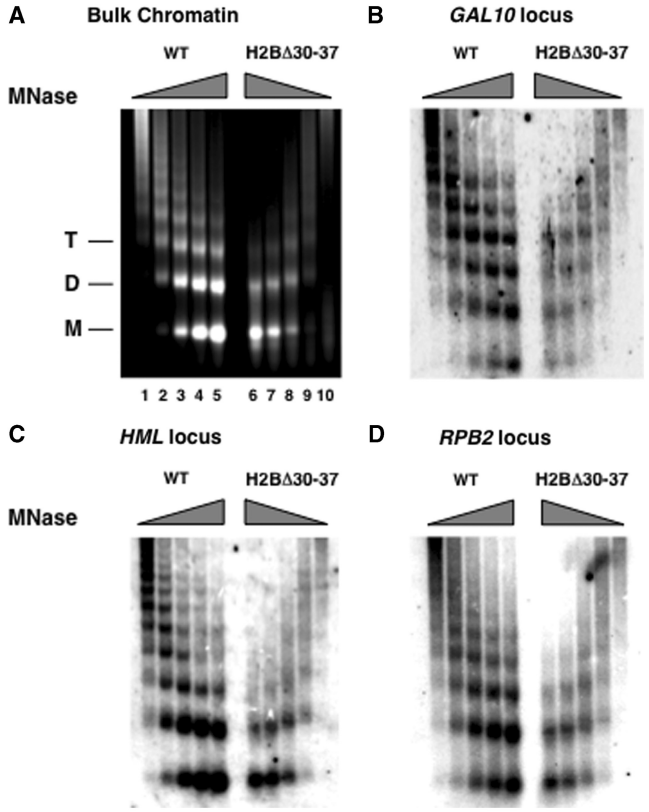

Figure 6. Locus-specific chromatin analysis. MNase digestion patterns for (**A**) Bulk chromatin, stained with ethidium bromide. M, D and T denote mono-, di- and tri-nucleosome DNA populations, respectively. Southern blot hybridizations performed with probes to the (**B**) *GAL10* (**C**) *HML* and (**D**) *RPB2* loci, respectively.

chromatin show distinct sub-monomer bands (i.e. <145 bp) at lower extents of digestion than *wt* or H2B Δ3–32 chromatin. These results indicate that deletion of amino acids 30–37 from the H2B N-terminal tail increases accessibility within the nucleosome.

Southern blot analyses with probes specific to the *GAL10, HML* or *RPB2* loci are shown in Figure 6B–D. These results indicate that, similar to bulk chromatin (Figure 6A), nucleosomes in these specific regions of H2B Δ30–37 mutant chromatin are also more accessible than *wt* nucleosomes.

Nucleosome occupancy in the silenced *HML* locus of H2B Δ30–37 mutant cells

The increase in DNA accessibility observed by MNase digestion of H2B Δ30–37 mutant chromatin could be due to changes in nucleosome occupancy rather than changes in DNA protection or nucleosome positioning. To address this possibility, we performed ChIP analysis of three regions within the *HML* locus and quantitatively determined the levels of both histone H2B and histone H3 occupancy. As shown in Figure 7, the level of histones H2B and H3 at all three regions is essentially equivalent in the H2B Δ30–37 mutant strain relative to the *wt* strain. Thus, the differences in MNase digestion patterns observed in Figure 6B for the *HML* locus are not likely to be a consequence of changes in nucleosome occupancy in this region.

Recruitment of Snf5 during NER in H2B Δ30–37 cells

It was previously reported that Snf5, a subunit of the Swi/Snf complex, interacts with histone H2B *in vivo*, and that

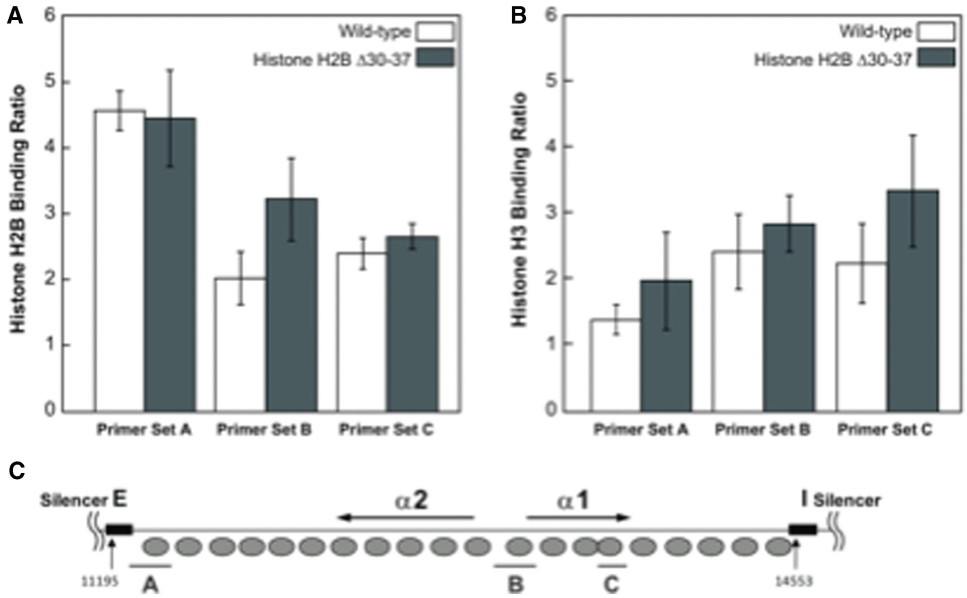

Figure 7. Histone occupancy at the *HML* locus in H2B Δ30–37 cells. ChIP was used to measure (**A**) histone H2B and (**B**) histone H3 occupancy levels at three locations within the *HML* locus. Error bars denote ±1 SD of the mean of three different experiments. No statistically significant differences in H2B or H3 levels were observed between *wt* and H2B Δ30–37 cells ($P > 0.05$). (**C**) Schematic of the yeast *HML* locus, including positions of nucleosomes (gray ovals) and primer sets used for ChIP experiments (horizontal lines A, B and C). Vertical arrows indicate the locations on chromosome III.

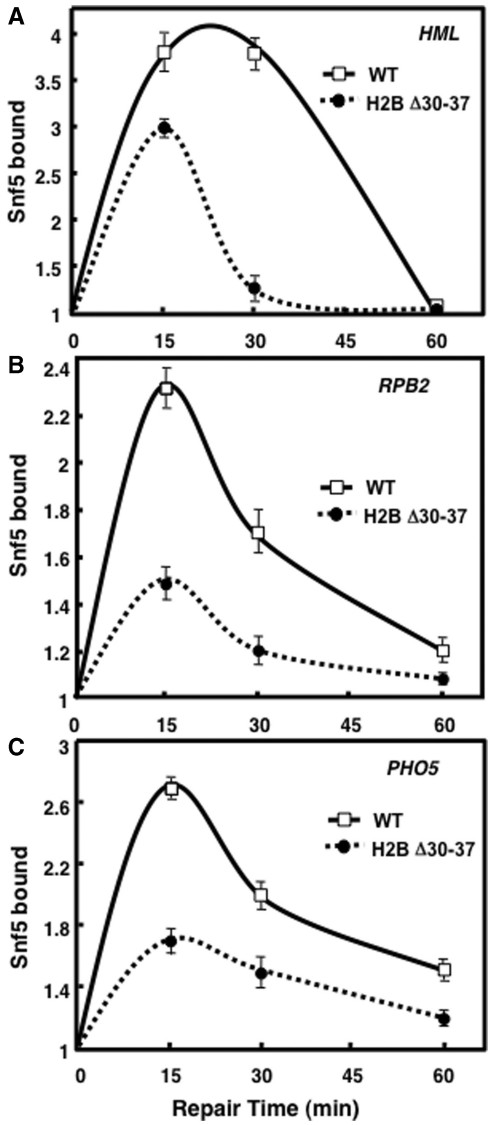

Figure 8. Recruitment of Snf5 to specific chromatin loci during NER. ChIP analysis of Snf5 protein recruitment to distinct chromatin regions of *wt* and H2B Δ30–37 cells during NER. Cells were UV irradiated and incubated for different repair times. Chromatin was immunoprecipitated with antibody specific to Snf5, followed by quantitative PCR amplification using gene-specific primers. Graphical representation of Snf5 occupancy in the *HML*, *RPB2* and *PHO5* loci are shown in (**A, B** and **C**), respectively. Snf5 recruitment during repair was normalized to the Snf5 occupancy at 0 h of repair. For each strain, data represent the mean ± 1 SD for three independent experiments.

H2B N-terminal deletion mutants can bypass the requirement for Swi/Snf during transcription (17). Furthermore, we have shown there is a direct association of Snf5 and Snf6 subunits of the SWI/SNF complex with the Rad4-Rad23 heterodimer in yeast (30). This heterodimer is a damage recognition complex in NER, and its interaction with Swi/Snf is stimulated by UV irradiation (30). Therefore, it is possible that during NER, interactions between nucleosomes and Swi/Snf are altered in H2B Δ30–37 mutant cells. We examined recruitment of Snf5 during NER to three different chromatin loci of UV-irradiated *wt* and H2B Δ30–37 cells, using ChIP analysis with Snf5 specific antibody followed by gene-specific linear PCR amplification. As shown in Figure 8, during NER Snf5 recruitment to all three loci of the H2B Δ30–37 mutant cells was more transient compared to *wt* cells. In the transcriptionally silent and nucleosome loaded *HML* locus, Snf5 occupancy in the H2B Δ30–37 mutant cells dropped sharply after 15 min of repair as opposed to *wt* cells (Figure 8A). Conversely, significant levels of Snf5 are present even after 30 min of repair in *wt* cells, after which there is a steady decline.

In the constitutively active *RPB2* region, the initial level of Snf5 recruitment is less in the H2B Δ30–37 mutant chromatin compared to *wt*, although Snf5 occupancy declines after 15 min of repair in both cell types (Figure 8B). In addition, it has been shown that chromatin remodeling in the inducible *PHO5* locus is mediated by the Swi/Snf complex along with other chromatin regulators (31). Therefore, we also tested Snf5 recruitment in the *PHO5* locus of the mutant cells during NER. In this locus, the initial recruitment of Snf5 was lower in the H2B Δ30–37 mutant cells (∼1.7) compared to *wt* (∼2.7), similar to the *RPB2* locus, with Snf5 occupancy declining after 15 min of repair (Figure 8C). Furthermore, we found comparable levels of Snf5 protein in H2B Δ30–37 and *wt* cells, and the level remained constant for at least the first 30 min of NER (Supplementary Figure S1). This result suggests that the reduced Snf5 recruitment in H2B Δ30–37 cells is not due to differences in the Swi/Snf protein level. Taken together these results indicate that during NER, Snf5 occupancy in specific loci of the H2B Δ30–37 mutant chromatin is reduced compared to *wt*, and is more transient at the *HML* locus. This could reflect an impaired docking of the H2B Δ30–37 nucleosomes with the Swi/Snf complex.

DISCUSSION

Deletion of residues 30–37 from the histone H2B N-terminus was earlier reported to confer significant UV-sensitivity (19). In trying to decipher the underlying cause for this phenotype, we examined NER in three specific chromatin loci: *HML*, *RPB2* and *GAL10*. When compared to *wt* cells, the H2B Δ30–37 mutant strain exhibits decreased NER in each of the loci tested (Figure 1). Reduced NER could be due to (i) increased DNA damage, (ii) decreased transcription of NER genes and/or (iii) altered chromatin structure that affects access to DNA damage as well as damage induction. Microarray analyses done previously on H2B Δ30–37 cells indicate that this deletion does not cause down-regulation of the known NER genes [(19); GEO series accession number GSE3806]. The reduced NER rate observed in H2B Δ30–37 cells could therefore be due to an increased damage level and/or altered chromatin structure. When CPD levels were tested, we found that the H2B Δ30–37 cells acquire more lesions in each of the chromatin loci mentioned above (Figure 2). Moreover, the H2B Δ30–37 cells were found to have more UV-induced lesions, both CPDs and (6-4) PPs, in the genome after the same UV dose (Figure 3). Therefore, the increased UV sensitivity

can be explained, at least in part, by increased DNA damage in the mutants.

Comparable DNA damage levels do not increase NER efficiency in the *HML* locus

The fact that H2B Δ30–37 cells acquire more UV-induced DNA damage, does not account for the reduced NER efficiency at the *HML* locus. NER in the mutant cells treated with a lower UV dose, where equal numbers of CPDs are generated, was found to remain lower than *wt* at this locus (Figure 4). On the other hand, NER in the *RPB2* and *GAL10* loci increased to *wt* levels after the lower UV dose. These results suggest that the increased UV sensitivity of H2B Δ30–37 cells is due to a combination of higher levels of UV-induced DNA damage and reduced efficiency of NER in at least condensed (or silenced) regions of chromatin.

Nucleosomes in H2B Δ30–37 mutant chromatin are more accessible and/or mobile

Chromatin structure is a strong determinant of DNA damage formation and repair kinetics (24,29,32). Deletion of core histone tail domains has been reported to affect nucleosome positioning, and consequently alter the accessibility of DNA target sites within nucleosomes (33). More specifically, deletion of the residues 30–37 of histone H2B has been shown to cause a significant decrease in plasmid superhelical density, most likely due to the release of constraints on DNA in nucleosomes (20). Consistent with these reports, our MNase results indicate that nucleosome DNA in H2B Δ30–37 chromatin is accessible over a larger 'linker-like' region (Figure 5). The nucleosome DNA ladders generated in the mutant chromatin are less distinct compared to *wt*, with more visible smears between the bands. Furthermore, the higher order nucleosome DNA bands are less prominent in the H2B mutant chromatin, especially in the more open chromatin regions of *RPB2* and *GAL10* (Figure 6A–D). These results suggest enhanced nucleosome mobility and/or higher access to a larger fraction of nucleosomal DNA in H2B Δ30–37 chromatin is due to less strongly positioned nucleosomes.

As depicted in the nucleosome crystal structure (Figure 9), amino acids 30–37 of histone H2B (in yellow) are located near the junction of the N-terminal tail and the first α-helix from the N-terminus. This cassette of amino acids pass between the two gyres of the DNA superhelix, bearing residues that are involved in direct interactions with the DNA (2). Therefore, it is possible that deletion of the proximal tail domain residues affect nucleosome positioning, and consequently alters nucleosome mobility and DNA accessibility (11,33). Moreover, H2B N-terminal tails, along with those of H2A, have been shown to interact with DNA of neighboring nucleosomes and mediate fiber-fiber interactions (3,34). Thus, it is possible that deletion of eight residues from the H2B N-tail also affects DNA stability within nucleosomes and higher-order chromatin structure. This altered chromatin 'landscape' in H2B Δ30–37 cells could be the primary cause of increased UV-induced DNA damage formation

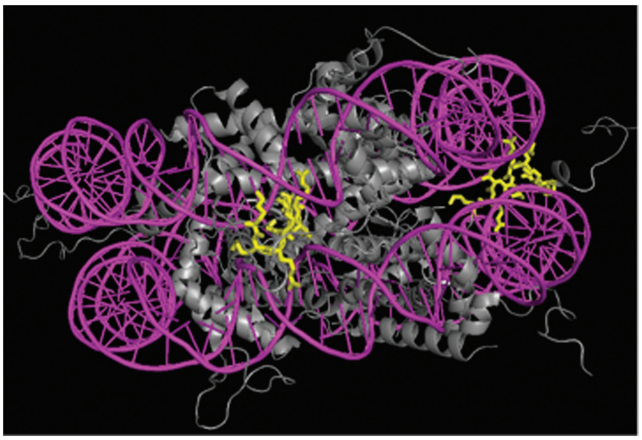

Figure 9. Location of H2B residues 30–37 in the nucleosome core structure. A side view of the nucleosome core particle structure is shown with the positions of histone H2B residues 30–37 (colored yellow) passing in between the two gyres of the DNA superhelix (colored purple). The image was drawn using PYMOL.

(Figures 2 and 3) and impaired NER rates (Figure 1) observed in these cells.

To further understand the relation between H2B N-terminal deletions and chromatin structure in H2B Δ3–37 cells, we performed MNase digestions with chromatin from the H2B Δ3–32 and H2B Δ3–37 cells. The UV sensitivity of H2B Δ3–32 cells has been shown to be similar to *wt* cells, while the H2B Δ3–37 cells have a lower survival rate, comparable to H2B Δ30–37 cells (19). Interestingly, we found that H2B Δ3–32 chromatin yields a distinct nucleosome ladder similar to *wt* chromatin, while H2B Δ3–37 chromatin digests are similar to those of H2B Δ30–37 (Figure 5B). Furthermore, analogous to H2B Δ30–37 chromatin, MNase digests of H2B Δ3–37 chromatin show distinct sub-monomer bands (i.e. <147 bp) at lower extents of digestion than *wt* or H2B Δ3–32 chromatin. Finally, we found no difference in H2B or H3 levels in HML chromatin of mutant and *wt* cells (Figure 7), indicating that the changes in nucleosome digestion profiles (Figure 6) do not reflect a change in nucleosome occupancy. Taken together, these results indicate that deletion of the 30–37 amino acid cassette in H2B increases internal nucleosome accessibility and/or nucleosome mobility.

Deletion of residues 30–37 of histone H2B does not generate a 'SIN' phenotype

A previous study indicates that Snf5, a subunit of the Swi/Snf complex, interacts with histone H2B *in vivo* (17). The authors have suggested that Swi/Snf might work to alter histone–DNA interactions by targeting the histone H2B N-terminus directly or indirectly through one or more histone protein(s). In agreement, we find that the overall binding of Snf5 at three different chromatin loci following UV irradiation is reduced and shorter lived in H2B Δ30–37 mutant cells during NER (Figure 8). In the nucleosome-loaded *HML* locus of H2B Δ30–37 cells, Snf5 occupancy is very transient and there is a sharp decrease in Snf5 binding at earlier repair times than in

wt cells (Figure 8A). On the other hand, the more open chromatin regions *RPB2* and *PHO5* show similar *kinetics* of Snf5 occupancy in the H2B Δ30–37 and *wt* cells during NER, although the initial level of Snf5 recruitment is distinctly less in the mutant cells (Figure 8B and C). We conclude that H2B Δ30–37 mutant nucleosomes cannot bind or recruit Snf5 as efficiently as the *wt* nucleosomes, in at least the silenced chromatin regions. We have shown previously that Swi/Snf remodeling is required for efficient NER in the transcriptionally silent *HML* locus of yeast cells (30). Our present results indicate that Snf5 binding is impaired in the *HML* locus of H2B Δ30–37 cells during NER. Taken together, it seems likely that the reduced repair rate observed in the *HML* locus, is due to inefficient recruitment and functioning of the Swi/Snf complex during NER.

It is also possible that recruitment of the silencing complex is altered by the H2B deletion. Indeed, reduced NER in the HML region could reflect increased levels of Sir protein binding in H2B Δ30–37 mutants. However, ChIP analyses of Sir4 protein levels at representative silenced regions (TEL V-L and TEL VI-R) show a significant *decrease* in Sir binding in the H2B Δ30–37 mutants relative to *wt* (M. Kyriss and J. Wyrick, manuscript in preparation). Therefore, it is unlikely that increased Sir binding is the cause of reduced NER in the HML domain of H2B Δ30–37 mutants. In addition, we found no evidence for an interaction between components of the Sir complex (Sir2, Sir3 or Sir4) with any component of the SWI/SNF remodeling complex (35). This, coupled with the observation that Swi/Snf levels are lower in the *HML* locus (Figure 8), also indicates that the reduced repair rate observed in this region is due to inefficient recruitment and functioning of the Swi/Snf complex during NER. On the other hand, nucleosomes in more open chromatin regions of H2B Δ30–37 cells, such as *RPB2* and *GAL10,* may not require Swi/Snf activity for efficient NER.

Deletion of residues 3–22 from the H2B N-terminus has been shown to confer a Sin (Swi/Snf independent) phenotype in the mutant cells (17). Our results, however, suggest that deletion of residues 30–37 of H2B generate a different phenotype than Sin. First, we have previously shown that the Sin mutation R45 of histone H4 renders yeast cells more *resistant* to UV damage (24). Second, the H4 R45 mutation *enhances* NER at the same chromatin loci (*HML*, *RPB2* and *GAL10*) studied in this report. Finally, our present results indicate chromatin remodeling by the Swi/Snf complex is required, but impaired, in the transcriptionally silent *HML* locus of H2B Δ30–37 cells. Thus, it seems that deletion of residues 30–37, located at the juncture of the N-terminal tail domain and the structured core domain (Figure 9), affects chromatin structure differently than the distal N-terminal tail residues 3–22.

The inefficiency in Snf5 recruitment by H2B Δ30–37 nucleosomes could be due to several possibilities. The shortening of the H2B N-tail by deletion of 8 amino acids may physically impede the docking of Swi/Snf. Since, deletion of residues 30–37 in H2B does not alter the level of histone H2B proteins (19), or the level of Snf5 protein (Supplementary Figure S1) in the mutant cells, disruption of the Swi/Snf interaction with H2B tails in H2B Δ30–37 nucleosomes is a distinct possibility. Alternatively, as H2B N-terminal tails harbor multiple sites of posttranslational modifications (36), the lack of these modification sites may affect chromatin modulation during NER. It was shown that the yeast H2B N-terminal tail has six lysine residues as potential acetylation sites, of which K22, K16 and K11 are most common, as well as a few sites of phosphorylation (S10) and sumoylation (K6/K7; K16/K17) (37–39). Unavailability of any of these sites in H2B 30–37 nucleosomes could affect chromatin accessibility, and consequently the dynamics of NER. Moreover, the 30–37 domain of histone H2B might itself have yet unidentified sites of posttranslational modifications which could affect chromatin structure. Clearly, investigation of the cause of defective Snf5 binding by the H2B Δ30–37 nucleosomes is of interest for future studies.

Finally, *in vitro* studies have indicated that the N-terminus of histone H2B is specifically required for chromosome condensation (40). However, there are very few *in vivo* studies showing how the histone H2B N-terminus regulates chromatin structure and function. In this report, we have shown that deletion of 8 amino acid residues (33–40) from the histone H2B N-terminal domain causes reduced NER efficiency in specific chromatin loci of yeast cells. This deletion yields more UV damage to the DNA of mutant cells and less efficient Snf5 recruitment, which solely (or cumulatively) affects NER efficiency in these cells. Taken together, this study reveals another important aspect of histone H2B N-terminal domains in regulating chromatin structure and function.

SUPPLEMENTARY DATA

Supplementary Data are available at NAR Online.

ACKNOWLEDGEMENTS

We thank Drs Anamaria Zavala and Shubho Chaudhuri from the Smerdon lab for critically evaluating this article.

FUNDING

National Institutes of Health (ES004106 to M.J.S.); American Cancer Society (RSG-03-181-01-GMC to J.J.W.). Funding for open access charge: National Institutes of Health (grant ES004106).

Conflict of interest statement. Its contents are solely the responsibility of the authors and do not necessarily represent the official views of the NIEHS, NIH.

REFERENCES

1. Arents,G., Burlingame,R.W., Wang,B.C., Love,W.E. and Moudrianakis,E.N. (1991) The nucleosomal core histone octamer at 3.1 A resolution: a tripartite protein assembly and a left-handed superhelix. *Proc. Natl Acad. Sci. USA*, **88**, 10148–10152.

2. Luger,K., Mader,A.W., Richmond,R.K., Sargent,D.F. and Richmond,T.J. (1997) Crystal structure of the nucleosome core particle at 2.8 A resolution. *Nature*, **389**, 251–260.
3. Zheng,C. and Hayes,J.J. (2003) Intra- and inter-nucleosomal protein-DNA interactions of the core histone tail domains in a model system. *J. Biol. Chem.*, **278**, 24217–24224.
4. Kouzarides,T. (2007) Chromatin modifications and their function. *Cell*, **128**, 693–705.
5. Allis,C.D., Jenuwein,T., Reinberg,D. and Caparros,M.L. (eds) (2007) *Epigenetics*. Cold Spring Harbor Laboratory Press, Cold Spring Harbor, NY.
6. Wolffe,A.P. and Hayes,J.J. (1999) Chromatin disruption and modification. *Nucleic Acids Res.*, **27**, 711–720.
7. He,H. and Lehming,N. (2003) Global effects of histone modifications. *Brief Funct. Genomic Proteomic*, **2**, 234–243.
8. Muthurajan,U.M., Park,Y.J., Edayathumangalam,R.S., Suto,R.K., Chakravarthy,S., Dyer,P.N. and Luger,K. (2003) Structure and dynamics of nucleosomal DNA. *Biopolymers*, **68**, 547–556.
9. Angelov,D., Vitolo,J.M., Mutskov,V., Dimitrov,S. and Hayes,J.J. (2001) Preferential interaction of the core histone tail domains with linker DNA. *Proc. Natl Acad. Sci. USA*, **98**, 6599–6604.
10. Fletcher,T.M. and Hansen,J.C. (1995) Core histone tail domains mediate oligonucleosome folding and nucleosomal DNA organization through distinct molecular mechanisms. *J. Biol. Chem.*, **270**, 25359–25362.
11. Hamiche,A., Kang,J.G., Dennis,C., Xiao,H. and Wu,C. (2001) Histone tails modulate nucleosome mobility and regulate ATP-dependent nucleosome sliding by NURF. *Proc. Natl Acad. Sci. USA*, **98**, 14316–14321.
12. Ferreira,H., Somers,J., Webster,R., Flaus,A. and Owen-Hughes,T. (2007) Histone tails and the H3 alphaN helix regulate nucleosome mobility and stability. *Mol. Cell Biol.*, **27**, 4037–4048.
13. Yang,Z., Zheng,C. and Hayes,J.J. (2007) The core histone tail domains contribute to sequence-dependent nucleosome positioning. *J. Biol. Chem.*, **282**, 7930–7938.
14. Somers,J. and Owen-Hughes,T. (2009) Mutations to the histone H3 alpha N region selectively alter the outcome of ATP-dependent nucleosome-remodelling reactions. *Nucleic Acids Res.*, **37**, 2504–2513.
15. Sivolob,A., Lavelle,C. and Prunell,A. (2003) Sequence-dependent nucleosome structural and dynamic polymorphism. Potential involvement of histone H2B N-terminal tail proximal domain. *J. Mol. Biol.*, **326**, 49–63.
16. Davey,C.A., Sargent,D.F., Luger,K., Maeder,A.W. and Richmond,T.J. (2002) Solvent mediated interactions in the structure of the nucleosome core particle at 1.9 a resolution. *J. Mol. Biol.*, **319**, 1097–1113.
17. Recht,J. and Osley,M.A. (1999) Mutations in both the structured domain and N-terminus of histone H2B bypass the requirement for Swi-Snf in yeast. *EMBO J.*, **18**, 229–240.
18. Ujvari,A., Hsieh,F.K., Luse,S.W., Studitsky,V.M. and Luse,D.S. (2008) Histone N-terminal tails interfere with nucleosome traversal by RNA polymerase II. *J. Biol. Chem.*, **283**, 32236–32243.
19. Parra,M.A., Kerr,D., Fahy,D., Pouchnik,D.J. and Wyrick,J.J. (2006) Deciphering the roles of the histone H2B N-terminal domain in genome-wide transcription. *Mol. Cell Biol.*, **26**, 3842–3852.
20. Lenfant,F., Mann,R.K., Thomsen,B., Ling,X. and Grunstein,M. (1996) All four core histone N-termini contain sequences required for the repression of basal transcription in yeast. *EMBO J.*, **15**, 3974–3985.
21. Bohr,V.A., Smith,C.A., Okumoto,D.S. and Hanawalt,P.C. (1985) DNA repair in an active gene: removal of pyrimidine dimers from the DHFR gene of CHO cells is much more efficient than in the genome overall. *Cell*, **40**, 359–369.
22. Mellon,I., Spivak,G. and Hanawalt,P.C. (1987) Selective removal of transcription-blocking DNA damage from the transcribed strand of the mammalian DHFR gene. *Cell*, **51**, 241–249.
23. Sweder,K.S. and Hanawalt,P.C. (1992) Preferential repair of cyclobutane pyrimidine dimers in the transcribed strand of a gene in yeast chromosomes and plasmids is dependent on transcription. *Proc. Natl Acad. Sci. USA*, **89**, 10696–10700.
24. Nag,R., Gong,F., Fahy,D. and Smerdon,M.J. (2008) A single amino acid change in histone H4 enhances UV survival and DNA repair in yeast. *Nucleic Acids Res.*, **36**, 3857–3866.
25. Mori,T., Nakane,M., Hattori,T., Matsunaga,T., Ihara,M. and Nikaido,O. (1991) Simultaneous establishment of monoclonal antibodies specific for either cyclobutane pyrimidine dimer or (6-4)photoproduct from the same mouse immunized with ultraviolet-irradiated DNA. *Photochem. Photobiol.*, **54**, 225–232.
26. Kuo,M.H. and Allis,C.D. (1999) In vivo cross-linking and immunoprecipitation for studying dynamic Protein:DNA associations in a chromatin environment. *Methods*, **19**, 425–433.
27. Chaudhuri,S., Wyrick,J.J. and Smerdon,M.J. (2009) Methylated lysine residues of histone H3 are required for efficient DNA repair at a silenced chromatin locus in *Saccharomyces cerevisiae*. *Nucleic Acids Res.*, **37**, 1690–1700.
28. Jin,Y., Rodriguez,A.M. and Wyrick,J.J. (2009) Genetic and genomewide analysis of simultaneous mutations in acetylated and methylated lysine residues in histone H3 in *Saccharomyces cerevisiae*. *Genetics*, **181**, 461–472.
29. Smerdon,M.J. and Conconi,A. (1999) Modulation of DNA damage and DNA repair in chromatin. *Prog. Nucleic Acid Res. Mol. Biol.*, **62**, 227–255.
30. Gong,F., Fahy,D. and Smerdon,M.J. (2006) Rad4-Rad23 interaction with SWI/SNF links ATP-dependent chromatin remodeling with nucleotide excision repair. *Nat. Struct. Mol. Biol.*, **13**, 902–907.
31. Steger,D.J. and O'Shea,E.K. (2004) Genetic analysis of chromatin remodeling using budding yeast as a model. *Methods Enzymol.*, **377**, 55–60.
32. Gong,F., Kwon,Y. and Smerdon,M.J. (2005) Nucleotide excision repair in chromatin and the right of entry. *DNA Repair*, **4**, 884–896.
33. Polach,K.J., Lowary,P.T. and Widom,J. (2000) Effects of core histone tail domains on the equilibrium constants for dynamic DNA site accessibility in nucleosomes. *J. Mol. Biol.*, **298**, 211–223.
34. Arya,G. and Schlick,T. (2006) Role of histone tails in chromatin folding revealed by a mesoscopic oligonucleosome model. *Proc. Natl Acad. Sci. USA*, **103**, 16236–16241.
35. Stark,C., Breitkreutz,B.J., Reguly,T., Boucher,L., Breitkreutz,A. and Tyers,M. (2006) BioGRID: a general repository for interaction datasets. *Nucleic Acids Res.*, **34**, D535–D539.
36. Wyrick,J.J. and Parra,M.A. (2009) The role of histone H2A and H2B post-translational modifications in transcription: A genomic perspective. *Biochim. Biophys. Acta*, **1789**, 37–44.
37. Jiang,L., Smith,J.N., Anderson,S.L., Ma,P., Mizzen,C.A. and Kelleher,N.L. (2007) Global assessment of combinatorial post-translational modification of core histones in yeast using contemporary mass spectrometry. LYS4 trimethylation correlates with degree of acetylation on the same H3 tail. *J. Biol. Chem.*, **282**, 27923–27934.
38. Ahn,S.H., Cheung,W.L., Hsu,J.Y., Diaz,R.L., Smith,M.M. and Allis,C.D. (2005) Sterile 20 kinase phosphorylates histone H2B at serine 10 during hydrogen peroxide-induced apoptosis in S. cerevisiae. *Cell*, **120**, 25–36.
39. Nathan,D., Ingvarsdottir,K., Sterner,D.E., Bylebyl,G.R., Dokmanovic,M., Dorsey,J.A., Whelan,K.A., Krsmanovic,M., Lane,W.S., Meluh,P.B. *et al.* (2006) Histone sumoylation is a negative regulator in Saccharomyces cerevisiae and shows dynamic interplay with positive-acting histone modifications. *Genes Dev.*, **20**, 966–976.
40. de la Barre,A.E., Angelov,D., Molla,A. and Dimitrov,S. (2001) The N-terminus of histone H2B, but not that of histone H3 or its phosphorylation, is essential for chromosome condensation. *EMBO J.*, **20**, 6383–6393.